# Spin flip in resonant photoemission from Gd

Z. Hu and K. Starke*
*Institut für Experimentalphysik, Freie Universität Berlin, Arnimallee 14, D-14195 Berlin-Dahlem, Germany*

G. van der Laan
*Daresbury Laboratory, Warrington WA4 4AD, United Kingdom*

E. Navas, A. Bauer, E. Weschke, C. Schüßler-Langeheine, E. Arenholz, A. Mühlig, and G. Kaindl
*Institut für Experimentalphysik, Freie Universität Berlin, Arnimallee 14, D-14195 Berlin-Dahlem, Germany*

J. B. Goodkoep and N. B. Brookes
*European Synchrotron Radiation Facility, Boîte Postale 220, F-38043 Grenoble Cedex, France*
(Received 20 January 1999)

We report the observation and theoretical analysis of magnetic circular dichroism of low-spin Gd $4f$ photoemission (PE) lines in the Gd $M_5$ photoexcitation region. With circularly polarized x rays tuned to previously unresolved absorption lines of magnetized Gd metal, low-spin and high-spin $4f$ PE lines become nearly equally strong. The observations are in excellent agreement with a state-of-the-art atomic multiplet calculation proving that spin-flip processes in resonant PE from lanthanides occur predominantly during the photoexcitation step. [S0163-1829(99)15815-6]

In atomic, molecular, and solid-state physics, x-ray absorption (XA) and core-level photoemission (PE) have greatly contributed to the present understanding of electron correlation, especially in transition metals with narrow valence bands and in lanthanides (Ln) with an incompletely filled $4f$ shell.[1] In order to enhance the PE cross section in an element-specific way, spectroscopists often use *resonant PE*, where they tune the photon energy to an XA line associated with the photoexcitation of an inner-core electron into a partially filled outer shell.[2] For a Ln atom in the ground-state configuration $4f^m$, resonant $4f$ PE can be written as

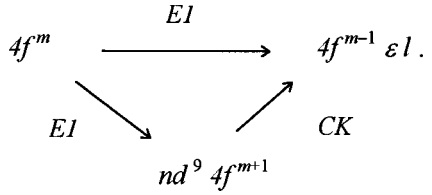


(1)

In addition to the *direct* electric-dipole excitation ($E1$) to continuum states, there is an *indirect channel* along which the same total final-state configuration, $4f^{m-1}\varepsilon l$, can be reached via an ''intermediate'' $d$-hole state ($n=3$ or 4) populated via $E1$; it decays through a *Coster-Kronig* Auger (CK) recombination, governed by Coulomb interaction between the intermediate $d$-hole state and the total final state. The coherent superposition of both channels is termed *resonant PE*; it is described by Fano's theory,[3] and constitutes a textbook example of quantum interference.[4]

Though resonant PE is widely used, the process itself is subject of considerable debate,[5–11] and in particular, the role of *spin flips* is still not clarified.[5–7] In spin-flip excitations, the spin $S'$ of the *total* final state, comprising the PE final state $4f^{m-1}$ and the associated continuum state $\varepsilon l$, differs from the ground-state spin $S$, i.e., $\Delta S \neq 0$. Since the $E1$ operator does not act in spin space, spin flips are forbidden in off-resonance PE. Yet in resonant PE, transitions with $\Delta S \neq 0$ may occur because $S$ is no longer a good quantum number, due to inner-shell spin-orbit coupling of the intermediate core-hole state.

Since the discovery of spin flips in 1981,[5] little progress has been made in their understanding. In particular, it has been debated whether they occur (i) primarily in the $d \rightarrow f$ excitation or (ii) in the CK recombination of the $d$-hole state. Several experimental efforts have been reported to clarify this question. It was realized that *low-spin* PE lines in the Gd $4f$ spectrum do not appear at the energies of all XA lines in the Gd $M_{4,5}$ (Ref. 6) and $N_{4,5}$ resonance[7] regions, an observation that led to conjecture (i): *spin flips* take place predominantly *in photoexcitation* and not so much in decay.[6] But direct measurement of the Gd $4f$ photoelectron spin polarization, comparing off-resonant with resonant PE at the $N_{4,5}$ XA threshold, indicated *equal spin polarizations* in both cases.[7] Thus hypothesis (ii) was brought up: *spin flips are absent* in resonant Gd $4f$ PE (at the main $N_{4,5}$ XA line), tentatively attributed to a *cancellation* of spin flips in the $E1$ and CK steps along the indirect resonance channel [see Eq. (1)].[7]

The present paper, based on a combined experimental and theoretical study of resonant PE using circularly polarized x rays in the $3d \rightarrow 4f$ threshold region of magnetically ordered Gd metal, demonstrates that spin-flip excitations leading to *low-spin* PE states occur *predominantly* during the photoexcitation step.

In our study of resonant $d \rightarrow f$ PE we employ magnetic circular dichroism, which has become possible through the availability of almost completely circularly polarized (CP) synchrotron radiation from the helical-undulator beamline ID 12-*B*/HELIOS-I at the European Synchrotron Radiation Fa-

 

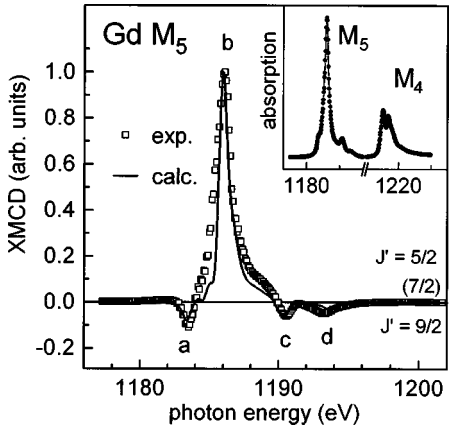


FIG. 1. High-resolution Gd $M_5$ XMCD spectrum. Minima at energies *a, c,* and *d* indicate the dominance of $J'=\frac{9}{2}$ core-hole excited states; the intense maximum *b* reflects the $J'=\frac{5}{2}$ character of the $M_5$ peak. Inset: XA spectrum across the whole $M_{4,5}$ spin-orbit doublet.

cility (ESRF). This beamline is designed particularly for high photon flux at energies from 500 to 1500 eV.[12] It is equipped with a spherical-grating monochromator (''dragon'' type), which maintains the high degree of circular polarization from the undulator; in the energy region around 1200 eV, ID 12-*B* supplies ~94% CP light[13] with a narrow energy width of $\Delta E=0.4\,\mathrm{eV}$ (resolving power, $E/\Delta E\cong 3000$; unprecedented for CP light in this photon-energy region).

Gd(0001) films were epitaxially grown on W(110) following a standard *in situ* procedure.[14] A thickness of $(10\pm 1)$ nm was chosen in order to ensure complete *in plane* magnetization at remanence and low coercivity (typically 200 Oe) for magnetization reversal by a low-field solenoid placed inside the UHV chamber. XA spectra were recorded in total electron yield; photoelectrons were collected around the surface normal by a hemispherical energy analyzer, operated in an angle-integrating mode (acceptance cone of ~20°) at 0.2-eV resolution. All XA and PE spectra were taken at an x-ray incidence angle of 30° with respect to the surface and a sample temperature of 30 K. The spectra were normalized to the incident photon flux and corrected for self-absorption, assuming an average electron-escape depth[15] of 2.0 nm and following the standard procedure of Thole *et al.*[16]

A high-resolution x-ray magnetic-circular-dichroism (XMCD) spectrum of Gd at the $M_5$ threshold is presented in Fig. 1, with the inset showing the XA spectrum across the whole $M_{4,5}$ spin-orbit doublet. The XMCD spectrum, which is the difference of the XA spectra measured for ''parallel'' and ''antiparallel'' orientation of photon spin and sample magnetization, clearly reveals weak structures below and above the main absorption line *b*. While energies and intensities of the XA spectrum were observed in numerous investigations at double-crystal monochromator beamlines,[16] the present observation of structures *a, c,* and *d* in the XMCD spectrum serves as a detailed experimental confirmation of the early prediction of *circular dichroism* at Ln $M_{4,5}$ edges.[17]

The sign of the XMCD signal in Fig. 1 is of particular significance. As pointed out previously, the $E1$-selection rules $\Delta M=+1$ and $\Delta M=-1$ for CP-light excitation lead preferentially to transitions with $\Delta J=-1$ and $\Delta J=+1$, respectively, in XA and PE from magnetized $4f$ systems.[18] Thus in magnetized Gd metal with an $^8S_{7/2}$ ground state, $|J=7/2,\ M=-7/2\rangle$, only intermediate states $|J'=9/2,\ M'=-9/2\rangle$ can be reached by a $\Delta M=-1$ transition. Therefore, a *negative* XMCD signal at energies *a, c,* and *d* (see Fig. 1) directly reveals a dominance of $J'=9/2$ intermediate states at these energies; analogously, the high *positive* XMCD of the main $M_5$ peak (*b*) reflects the presence of at least one strong $J'=5/2$ state. The total angular momentum $J'$, which due to $3d$-core spin-orbit coupling remains the only reasonably good quantum number to assign the intermediate $3d^94f^8$ states, can be simply ''read'' from the sign of the associated XMCD signal.

This picture is well supported by theoretical XA and PE spectra. They were calculated in intermediate coupling with Cowan's atomic multiplet code[4] using the relativistic Hartree-Fock-plus-statistical-exchange method. To properly include intra-atomic correlation effects in the metallic environment, Coulomb and exchange integrals were reduced to 84% of the atomic values,[19] resulting in good agreement with the experimental spectra. Radiative transitions were considered to first order ($E1$) and Coulomb interaction ($3d,4f;4f,\varepsilon l$) to infinite order. For the XA states, a lifetime broadening of 0.4 eV at $M_5$ was included to account for other autoionization channels besides the ($3d,4f;4f,\varepsilon l$) decay. Note that all parameters in the calculation (apart from the Slater integrals) were the same as used previously in Refs. 18 and 20. The calculated $M_5$ XMCD spectrum is given as solid curve in Fig. 1. The striking agreement with the experimental spectrum even in minute details lends strong support to the qualitative picture developed above and, in particular, confirms the $J'$ assignments obtained from the sign of the XMCD spectrum. With this reliable description of the *first* excitation step along the indirect channel [Eq. (1)], we turn to the resonance process as a whole.

Resonant Gd $4f$ PE spectra are presented in Fig. 2 for photon energies $a-d$ at the $M_5$ threshold as indicated in Fig. 1. Tuned to the main peak of the $M_5$ XA spectrum (*b*), the intensity of the $^7F$ line is about 20 times higher than at energies *a, c,* and *d*, reflecting the well-known enhancement of the $4f$ PE cross section at Ln $M_5$ edges.[6] The present use of CP light reveals large magnetic dichroism that, at *b*, amounts to an intensity asymmetry of over 60% in the $^7F$ PE line. This is equivalent to an extremely strong magnetic contrast, and might become a valuable tool in magnetic-domain imaging by PE microscopes (PEEM) using element-specific photoelectron signals instead of secondary electrons.

When tuning to the high-energy XA structures *c* and *d*, intense broad PE lines appear in the resonant $4f$ PE spectrum at binding energies (BE's) between 11 and 18 eV (cf. Fig. 2). In agreement with Refs. 5 and 6, they are identified as *low-spin* $4f$ PE lines $^5X$ comprising various orbital-momentum states *X*. These *low-spin* PE lines exhibit pronounced magnetic circular dichroism: for antiparallel orientation of magnetization and photon spin (filled circles), the total $^5X$ PE line intensity is nearly *equal* to the $^7F$ intensity, whereas for 'parallel' orientation (open circles), it reaches only half the intensity of the high-spin $^7F$ line at *c*, and only a quarter at *d*. The corresponding MCD spectra (difference spectra parallel minus antiparallel from Fig. 2) are shown in

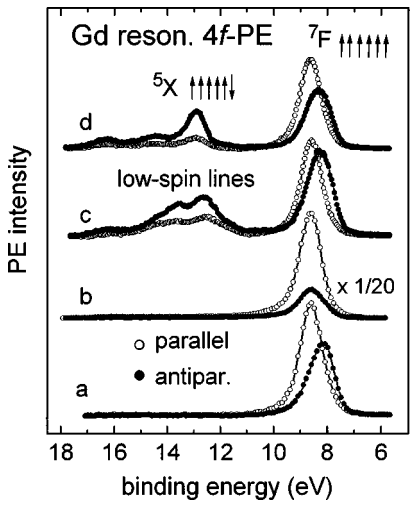


FIG. 2. Resonant $4f$PE spectra obtained with CP light from magnetized Gd at the $M_5$ threshold. Photoexcitation energies *a* to *d* are defined in Fig. 1. Open (closed) symbols refer to the photon momentum oriented nearly parallel (antiparallel) to the magnetization. At the $M_5$ peak (*b*), the PE intensity is scaled by $\frac{1}{20}$ for display. Arrows show single-electron *f*-spin orientations of the $4f^6$ low-spin ($^5X$) and high-spin ($^7F$) PE final states.

Fig. 3. At energies *c* and *d*, the MCD signal is *negative* in the whole $^5X$ region, opposite to the positive MCD of the $^7F$ PE line at the $M_5$ main peak (*b*).

For a first qualitative understanding of the observed MCD of the *low-spin* Gd $4f$ PE lines, we may neglect the direct photoexcitation channel. This is justified from the calculated dipole-matrix elements[19] indicating that, at photon energies of ~1.2 keV, $3d\rightarrow 4f$ $E1$ core-excitation is *four* orders of magnitude stronger than photoexcitation into the continuum—a dominance that is well reflected by the nearly Lorentzian line shapes[4] of Ln $M_5$ XA lines. In this approximation, resonant PE multiplet intensities are simply obtained by projecting the angular momenta of the intermediate states $3d^9\ 4f^8$ onto $4f^6$ PE final states and associated continuum

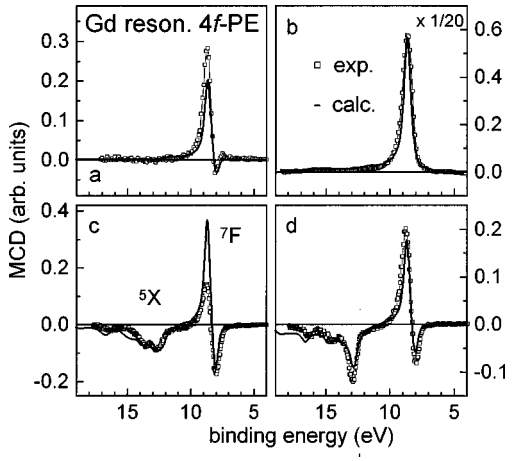


FIG. 3. Comparison of experimental (open squares) MCD signals, associated with the resonant $4f$ PE spectra from Fig. 2, with theoretical spectra (solid curves) at the given $M_5$ threshold energies. Note the overall *negative* MCD of $^5X$ PE *low-spin* lines (*c*,*d*) as opposed to the strongly positive MCD of the $^7F$ PE *high-spin* line at the $M_5$ peak (*b*).

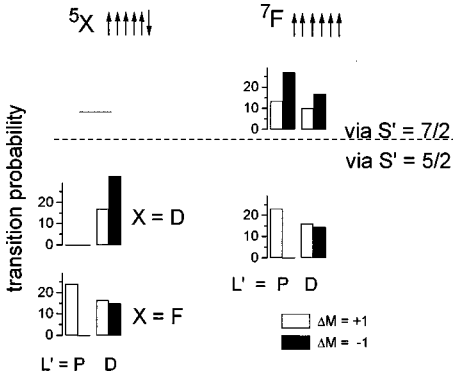


FIG. 4. Bar diagram of relative transition probabilities (arb. units) for resonant Gd $3d\rightarrow 4f$ PE, calculated in pure *LS* coupling. *Low-spin* $^5X$ PE final states (left) are reached only via low-spin ($S'=\frac{5}{2}$) intermediate states. (Primed symbols represent momenta of intermediate XA states.)

states $\varepsilon l$ ($l=d$ contributions are neglected at Gd $M_5$ photon energies). The simple basis transformation (''recoupling'') is readily achieved within the *LS* coupling scheme.[4,21]

Relative transition probabilities to Gd $4f^6$ PE final states are displayed in Fig. 4. It shows that the *high-spin* PE line $^7F$, with $S''=3$, can be reached via both *high-spin* $S'=\frac{7}{2}$ and *low-spin* $S'=\frac{5}{2}$ intermediate states. (Primed and double-primed symbols represent angular momenta of intermediate states and PE final states, respectively.) By contrast, *low-spin* PE states $^5X$, with $S''=2$, can only be populated via *low-spin* intermediate states. In other words: the spin flip needed to reach a *low-spin* PE state, from the $S=\frac{7}{2}$ ground state of Gd, must take place in the photoexcitation step along the indirect channel. The spin-flip question in $d\rightarrow f$ resonant PE can thus be answered as follows: In the limit of pure *LS* coupling, the photoelectron spin, $s=1/2$, is simply too small for populating a low-spin, $S''=2$, PE final state via a high-spin, $S'=\frac{7}{2}$, intermediate state. As revealed in Fig. 4 (bottom right), there is, however, a nonvanishing probability for resonant $3d\rightarrow 4f$ PE via *low-spin* intermediate states to *high-spin* $4f$ PE final states $^7F$.

These statements are strictly valid within the *LS* coupling scheme. Yet, the large spin-orbit interaction in Ln $3d$ shells does not only lift spin conservation (hereby allowing for spin-flip transitions), but prohibits also a labeling of the $3d^9\ 4f^8$ intermediate with a unique $L'S'$ pair of quantum numbers; instead, a complete $L'S'$ basis-function expansion is required. Thus, strictly speaking, the answer is that *low-spin* Gd $4f^6$ PE final states ($S''=2$) are populated significantly *only* via *low-spin* intermediate states ($S'=5/2$) of high purity.

This interpretation in the *LS*-coupling scheme is well supported by our intermediate-coupling calculations. In Fig. 3, theoretical resonant Gd $4f$ PE MCD spectra are included as solid lines for the four photon energies studied. In the calculation, the lifetime of the PE final state was taken as infinite; the spectra were convoluted by a Gaussian of $\sigma=85$ meV (for experimental broadening) and with a Doniach-Sunjic line (asymmetry parameter 0.1) with lifetime width $2\Gamma=360$ meV (600 meV) for the $^7F$ ($^5X$) lines. For display in Fig. 3, the calculated spectra were normalized to the experimental data at the main peak *b*. The relative size of the

MCD-PE signals is well reproduced at all excitation energies; in particular, there is excellent agreement in the resonant *high-spin* and *low-spin* signals.

Finally, we turn to the nearly equal intensities of *low-spin* and *high-spin* resonant $4f$ PE line in $\Delta M=-1$ transitions. Again, a qualitative understanding is obtained in *LS* coupling. From the full (intermediate coupling) calculation we know that the intermediate XA states are mainly *P* and *D* like. But, as is shown in Fig. 4, no $X=P$ *low-spin* PE states can be reached via $L'=P$ or *D*. PE states with $X=D$ are allowed, yet with a strong imbalance between $\Delta M=+1$ and $\Delta M=-1$ transitions: via $L'=D$-like intermediate states, the $^5X$ PE intensity with $X=D$ is about twice as intense for $\Delta M=-1$ than for $\Delta M=+1$. Also, there should be *no* $^5X$ intensity at all for $\Delta M=-1$ via a *P*-like state. Therefore, the negative MCD of the $^5X$ PE lines in Fig. 3—observed both experimentally and theoretically—reveals a dominant *D* character of the intermediate Gd $3d^9\,4f^8$ states at the energies *c* and *d*, and shows that the *low-spin* Gd $4f$ PE lines have mainly $X=D$ character.

In summary, the present work shows that the spin flip in $d\rightarrow f$ resonant PE from Ln materials, which leads to *low-spin* $4f$ PE lines, occurs predominantly in the photoexcitation step. In addition, the over 60% MCD of the resonantly enhanced *high-spin* Gd $4f$ PE line may become useful for magnetic domain imaging by next-generation PE microscopes.

This work was supported by the Bundesminister für Bildung, Wissenschaft, Forschung und Technologie, Project No. 05-SC8 KEB-6.

*Corresponding author. Electronic address: starke@physik.fu-berlin.de

[1] R. J. H. Kappert, H. R. Borsje, and J. C. Fuggle, J. Magn. Magn. Mater. **100**, 363 (1991).

[2] W. Lenth, F. Lutz, J. Barth, G. Kalkoffen, and C. Kunz, Phys. Rev. Lett. **41**, 1185 (1978).

[3] U. Fano, Phys. Rev. **124**, 1866 (1961).

[4] R. D. Cowan, *The Theory of Atomic Structure and Spectra* (University of California Press, Berkeley, 1981).

[5] F. Gerken, J. Barth, and C. Kunz, Phys. Rev. Lett. **47**, 993 (1981).

[6] C. Laubschat *et al.*, Phys. Scr. **41**, 124 (1990).

[7] T. Kachel *et al.*, Phys. Rev. B **45**, 7267 (1992).

[8] M. F. López, C. Laubschat, A. Gutiérrez, and G. Kaindl, Z. Phys. B **94**, 1 (1994).

[9] J.-J. Gallet *et al.*, Phys. Rev. B **54**, R14 238 (1996); C. Dallera *et al.*, *ibid.* **56**, 1279 (1997).

[10] M. Weinelt *et al.*, Phys. Rev. Lett. **78**, 967 (1997).

[11] S. R. Mishra *et al.*, Phys. Rev. Lett. **81**, 1306 (1998).

[12] J. Goulon *et al.*, Physica B **208/209**, 199 (1995).

[13] M. Drescher *et al.*, Rev. Sci. Instrum. **68**, 1943 (1997).

[14] J. Kolaczkiewicz and E. Bauer, Surf. Sci. **175**, 487 (1986).

[15] The electron-escape depth of 2.0 nm for saturation correction was determined experimentally using a monolayer of Eu grown on Gd(0001) [E. Arenholz *et al.*, Phys. Rev. Lett. **80**, 2221 (1998)], and comparing Gd $M_5$ and unsaturated Eu $M_5$ XA spectra.

[16] B. T. Thole *et al.*, Phys. Rev. B **32**, 5107 (1985).

[17] B. T. Thole, G. van der Laan, and G. A. Sawatzky, Phys. Rev. Lett. **55**, 2086 (1985); J. B. Goodkoep *et al.*, Phys. Rev. B **37**, 2086 (1988).

[18] K. Starke *et al.*, Phys. Rev. B **55**, 2672 (1997).

[19] The atomic Hartree-Fock values of the Slater integrals and spin-orbit parameters are given in Ref. 16 for XA, and in Ref. 20 for PE. The Coster-Kronig matrix elements are: $R(3d,4f;4f,\varepsilon s)=-0.0782\ \mathrm{eV}/\sqrt{\mathrm{Ry}}$; $R^k(3d,4f;4f,\varepsilon d)=-0.1369,\ 0.1237,\ 0.1012\ \mathrm{eV}/\sqrt{\mathrm{Ry}}$; $R^k(3d,4f;4f,\varepsilon g)=0.7132,\ 0.4647,\ 0.3337\ \mathrm{eV}/\sqrt{\mathrm{Ry}}$. The dipole matrix elements are $\langle 3d\|r\|4f\rangle=-0.228\ 33$ a.u.; $\langle 4f\|r\|\varepsilon d\rangle=0.001\ 53$ a.u./$\sqrt{\mathrm{Ry}}$; $\langle 4f\|r\|\varepsilon g\rangle=-0.01192$ a.u./$\sqrt{\mathrm{Ry}}$.

[20] G. van der Laan and B. T. Thole, Phys. Rev. B **48**, 210 (1993).

[21] The bar diagram (Fig. 4) can be obtained by using the expression given in Ref. 18 (with the $3j$ symbol squared).